Journal of the Korean Society for Nondestructive Testing
Vol. 28, No. 3 (2008. 6)

Neural Network Analysis of Acoustic Emission Signals for Drill Wear Monitoring

Kritsada Prasopchaichana* and Oh-Yang Kwon*†

Abstract The objective of the proposed study is to produce a tool-condition monitoring (TCM) strategy that will lead to a more efficient and economical drilling tool usage. Drill-wear monitoring is an important attribute in the automatic cutting processes as it can help preventing damages of the tools and workpieces and optimizing the tool usage. This study presents the architectures of a multi-layer feed-forward neural network with back-propagation training algorithm for the monitoring of drill wear. The input features to the neural networks were extracted from the AE signals using the wavelet transform analysis. Training and testing were performed under a moderate range of cutting conditions in the dry drilling of steel plates. The results indicated that the extracted input features from AE signals to the supervised neural networks were effective for drill wear monitoring and the output of the neural networks could be utilized for the tool life management planning.

Keywords: Neural Network, Back-Propagation, Drill Wear, Tool-Condition Monitoring (TCM)

1. Introduction

Various methods for tool-wear monitoring have been reported in the literature. Most of them are categorized by two main techniques (Li and Patri, 1999; Li and Wu, 2000a; Li, 2002). The first is the direct measurement of tool wear using optical methods, which can only be applied when cutting tools are not in process of cutting. The second is the indirect methods which measure the relationship between the tool condition and the signals acquired depending on the sensors used. Among these, acoustic emission (AE) appeared to be one of the most effective methods. The major advantage of AE monitoring is that the frequency range of AE signals can be much higher than the machine vibrations and environmental noise. In addition, it does not affect the cutting condition. But one of the most important features for AE signal is the additional signal processing which extract signal features from the signals detected under given cutting conditions (Li, 2002; Sun et al., 2004).

The relationship between AE signals and the tool wear condition is nonlinear so that the general mathematical relations cannot be used to map this relation (Li, 2002). Recent studies in the field of artificial neural networks have proven that they can be particularly useful in the modeling of nonlinear mapping and in the recognition of distinctive features from incomplete or chaotic input data (Abu-Mahfouz, 2005; Patra et al., 2007; Singh et al., 2006).

TCM is an indispensable component for the prevention of the damage in machine tools and workpieces and the optimization of tool usage in the automated machining. Drill wear condition is an important factor directly affecting the quality parameters of machined holes, such as hole roundness, centering, burr formation, and surface

Received: October 5, 2007, Revised: December 27, 2007, Accepted: January 30, 2008. * Department of Mechanical Engineering, Inha University, Incheon 402-751, South Korea, † Corresponding Author: okwon@inha.ac.kr

finish. Furthermore, under a certain cutting condition, wear development during drilling can reach the unacceptable levels, resulting in the damage of workpieces as well as machine tools and possibly in the production loss. Flank wear is widely used as the indication of the severity of drill wear condition. Its progressive process is caused by the intimate frictional contact and the temperature elevated at the interface between the drill and the workpiece. Flank wear can be measured by using the average and the maximum wear land size, V_B and V_{Bmax}, as shown in Fig. 1.

In this study, we have investigated the feasibility to use signals to train and test the neural networks for predicting the drill flank wear. Six neural network architectures were designed with the different groups of input features. The inputs were extracted features from AE signals such as root mean square (RMS) voltages of the decomposed signal by discontinuous wavelet transform (DWT) and mean absolute wavelet coefficients by continuous wavelet transform (CWT).

2. Experimental Procedure

Experiments were carried out on a machining center (HiMac-V100, Hyundai). Drills used were AISI M2 twist drills with diameter 6 mm and point angle of 118°. Workpieces were AISI 1055 steel plates of 120×120×25 mm. The hardness of plates was measured to 215 H_B. Two broadband AE sensors (B1025, Digital Wave) were mounted on the clamping fixture at the opposite side each other as shown in Fig. 2. AE activities during drilling tests were monitored and recorded by using an AE data acquisition board (Mistras2001, Physical Acoustics), with pre-amplification of 40 dB, band-pass filtering at 0.1-1.2 MHz and threshold of 50 dB (equivalent 31.6 mV). During each test, flank wear was measured by an optical microscope aided by a digital camera and an image processing software. Drilling tests were first performed at nine sets of cutting conditions with three cutting speeds (V = 22, 26, 30 m/min) and three feed rates (f = 0.13, 0.15, 0.17 mm/rev) without coolant, which were used for off-line training and testing. Three sets of cutting conditions were added later to check the validity of the neural networks with the features extracted from untrained data set. The cutting process was continued until the max. allowable flank wear of V_B = 0.3 mm or the complete failure of a drill.

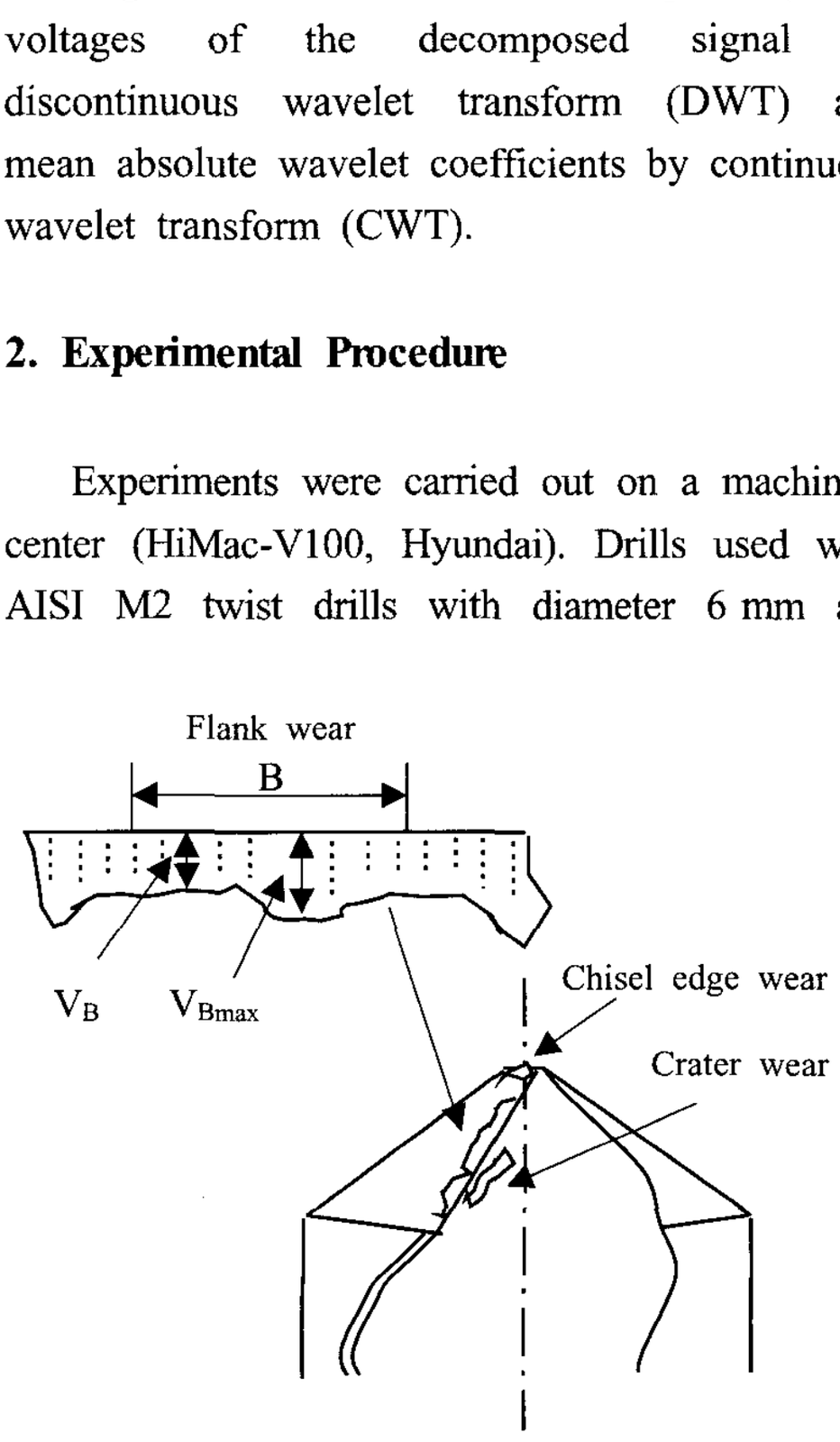

Fig. 1 Schematic of a typical twist drill with Flank wear

3. Signal Analysis and Feature Extraction

Based on the analysis of AE sources, AE signals detected from metal cutting consist of the continuous and the transient signals, which have distinctly different characteristics (Li, 2002). Continuous signals are associated with shearing

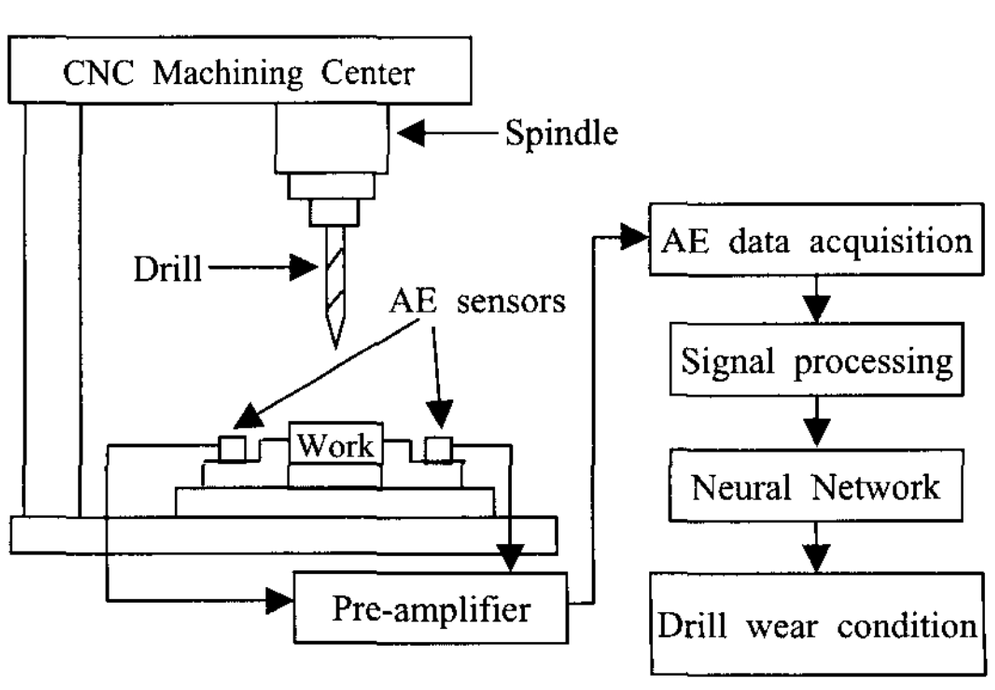

Fig. 2 Schematic diagram of the experiment set-up

in the primary zone and wear on the tool face and the flank, while transient or burst signals are with either tool fracture or chip breakage. In this study, the input features to the neural networks were extracted from the continuous AE signals at the drilling depth of 2-5 mm using level-RMS values by DWT analysis and mean absolute wavelet coefficients by CWT analysis.

3.1 Discrete Wavelet Transform Level-RMS Analysis

In the DWT analysis, the signal is decomposed to approximations and details. The approximations are the high-scale, low-frequency components of the signal and the details are the low-scale, high-frequency components. The decomposition process can be iterated, with successive approximations being decomposed in turn, so that one signal is broken down into many lower resolution components. This is called the wavelet decomposition tree as shown in Fig. 3 (Lee et al., 2000; Misiti, 2000). S represents raw AE signal; D_1, D_2,..., D_6 are details at level 1, 2, ..., 6 respectively; and A_6 means approximation at level 6.

DWT was applied to selected continuous AE signals to decompose the original AE signal into its wavelet levels as shown in Fig. 4. Each AE signal was decomposed to 7 wavelet levels, namely D_1, D_2,..., A_6 which are represented at frequency band [1-2], [1-0.5], ..., [0-0.03125] MHz, respectively. Because the AE signals were acquired at sampling rate of 4 MHz, frequencies up to 2 MHz were considered. Decomposition was based on 'db20' wavelet (member of the

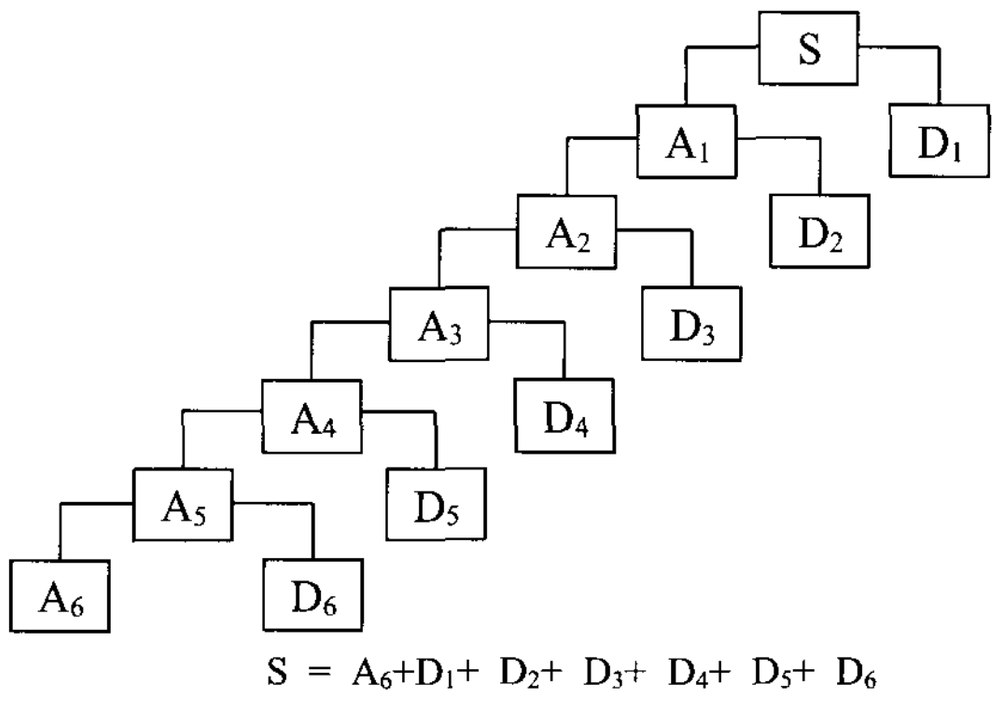

$S = A_6+D_1+ D_2+ D_3+ D_4+ D_5+ D_6$

Fig. 3 The 6-level wavelet decomposition tree

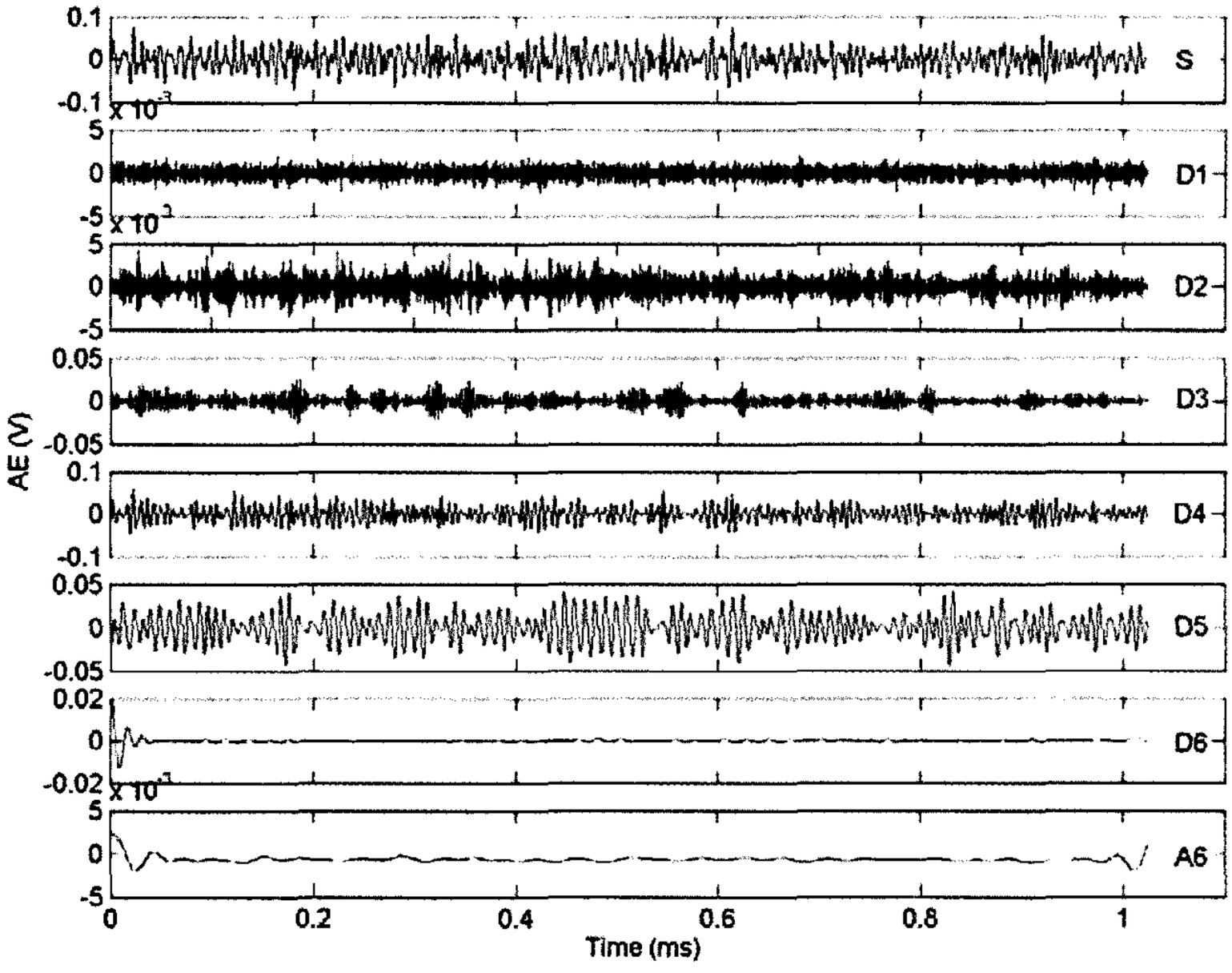

Fig. 4 Six-level wavelet decomposition of an AE signal

Daubechies wavelets family) and six levels of analysis. The RMS of each frequency band-level was used to describe the features of different tool condition (Li and Patri, 1999; Li and Wu, 2000a).

3.2 Continuous Wavelet Transform (CWT)

The CWT is defined as the sum over all time of the signal multiplied by scaled, shifted versions of the wavelet function. This process produces wavelet coefficients that are a function of scale and position. The CWT coefficients represent how closely correlated the wavelet is with this section of the signal. The higher CWT coefficient value is, the more the similarity. The CWT coefficient *C(a,b)* of a signal *f(t)* is defined by (Abu-Mahfouz, 2005; Misiti, 2000)

$$C(a,b) = \int_{-\infty}^{\infty} f(t)\frac{1}{\sqrt{a}}\psi^{*}(\frac{t-b}{a})dt \qquad (1)$$

where a presents scale, b represents position and ψ is the "mother" wavelet. ψ^{*} is the complex conjugate of ψ.

A member of Daubechies wavelets family, "db20" was selected as the mother wavelet for CWT in this study. In Fig. 5, three-dimensional plots of CWT coefficients for two cases of drill wear are presented in 8 scales (scale 4, 8, 12, …, 32). The 8 mean absolute CWT coefficients were determined and used to describe the changing feature of the AE signals which appeared to be influenced by the wear size and cutting conditions as shown in Fig. 6.

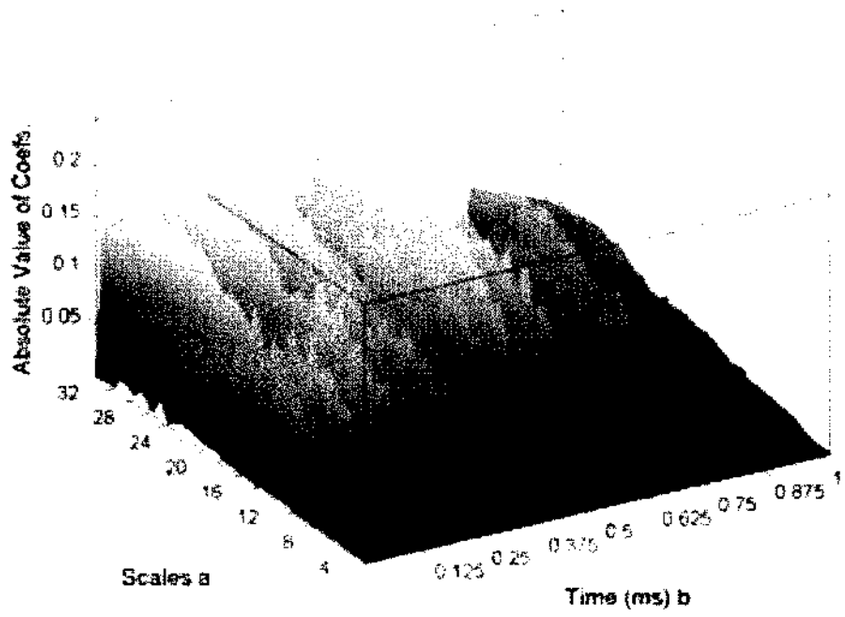

(a) V_B = 0.000 mm

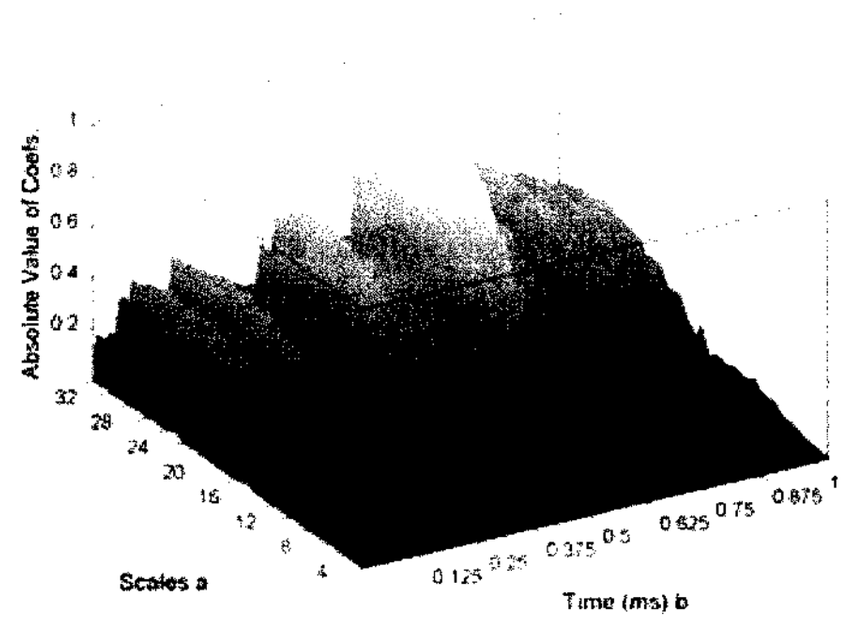

(b) V_B = 0.219 mm

Fig. 5 3D CWT coefficients surface for two cases of drill wear at cutting speed 26 m/min and feed 0.13 mm/rev

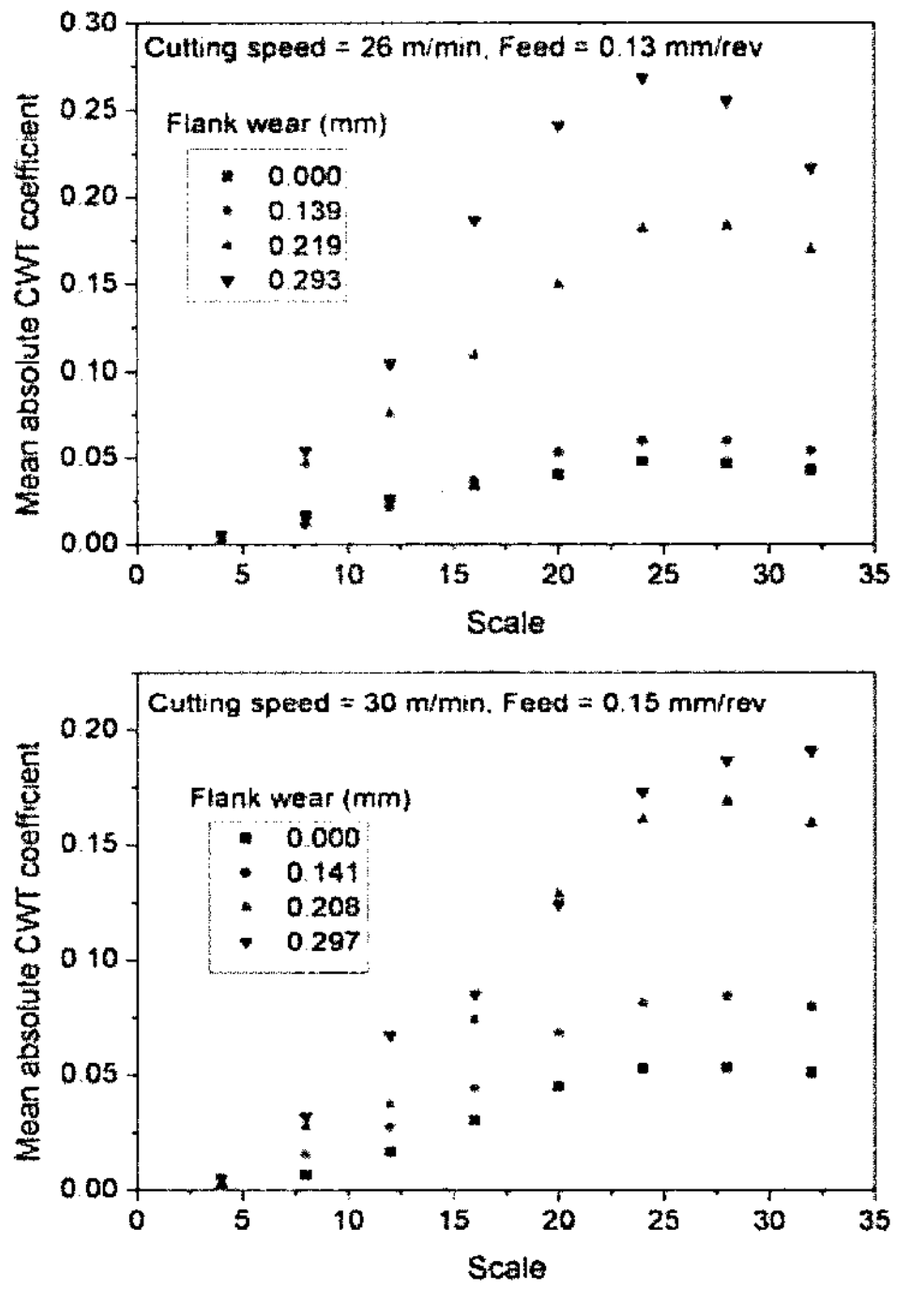

Fig. 6 The mean absolute 8 CWT coefficient scales for four progressive flank wear values at two cutting conditions

4. Neural Networks

The architecture of a four-layer feed-forward neural network (Kim and Lee, 2001; Patra et al., 2007; Singh et al., 2006) was used in this study. This neural network used a hyperbolic-tangent sigmoid transfer function, which is a good trade off for the neural networks where speed is important and the exact

shape of the transfer function is not (Demuth and Beale, 1998). In this study, the Levenberg-Marquardt algorithm (numerical optimization technique of backpropagation algorithm) is used in training neural networks in order to obtain neural networks with good generalization capability. This algorithm appears to be the fastest method for training moderate-sized feed-forward neural networks (Demuth and Beale, 1998). The learning process was stopped (i.e., neural network had converged) when the calculated output values were close to the desired target values within an acceptable mean-square error (MSE) value ($MSE < MSE_{goal} = 10^{-5}$).

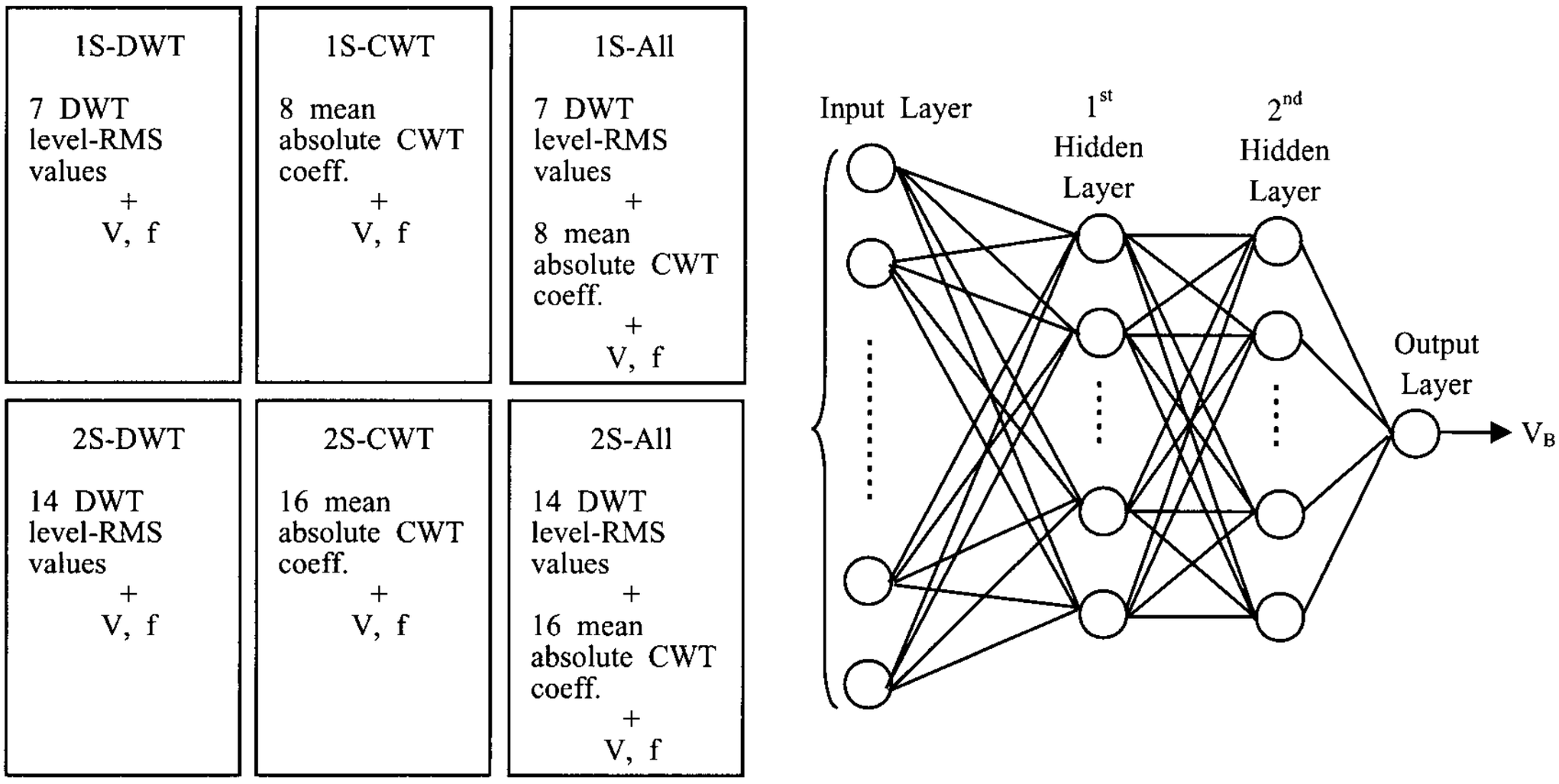

Fig. 7 Six neural network architectures

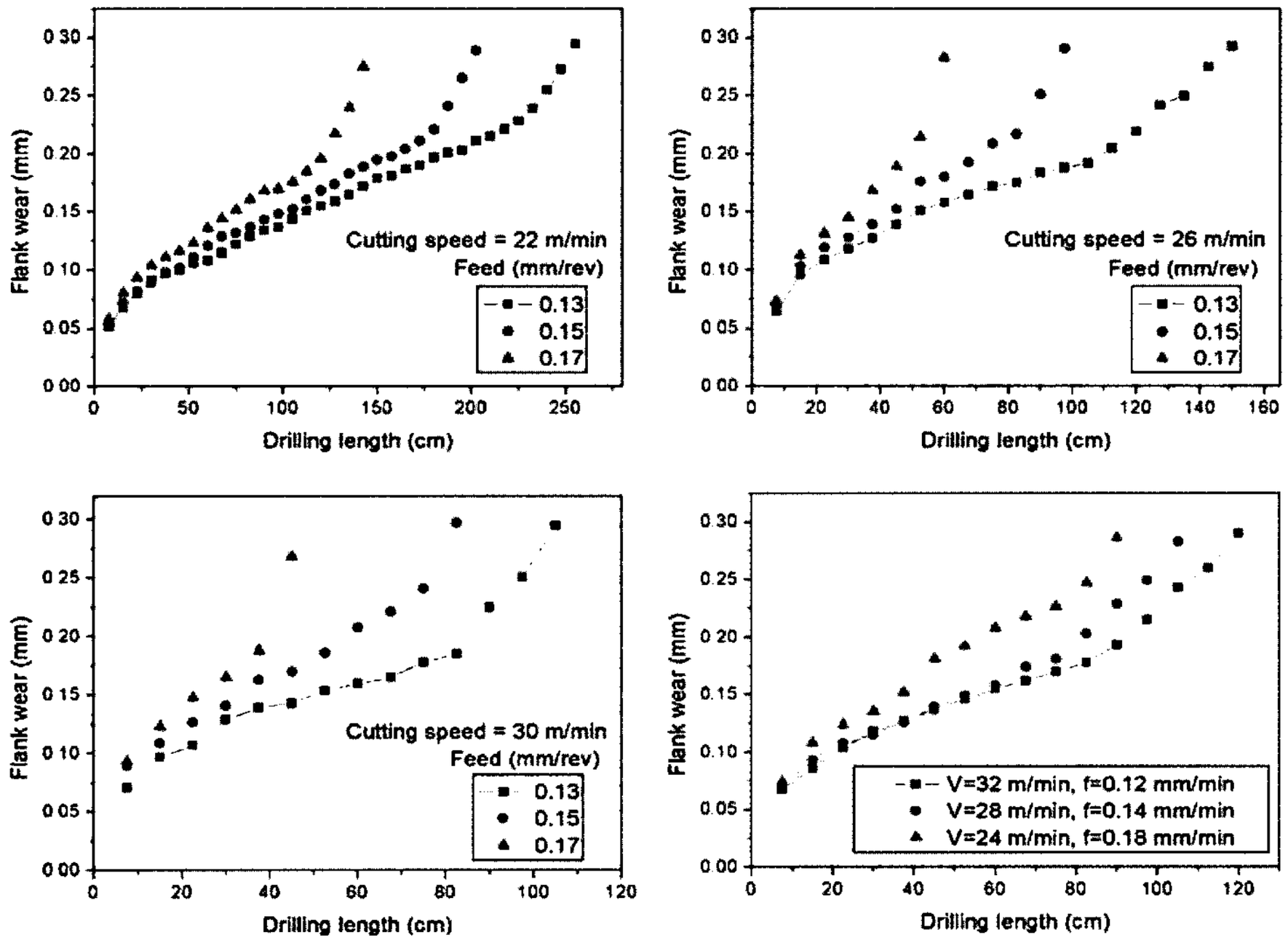

Fig. 8 Drill flank wear size measured during complete useful life

Six neural network architectures, shown in Fig. 7, were designed as follows:

1) 1S-DWT: Input 7 DWT level-RMS values of AE signals from only one sensor and cutting conditions.
2) 1S-CWT: Input 8 mean absolute CWT coefficients of AE signals from only sensor and cutting conditions.
3) 1S-All: Input 7 DWT level-RMS values and 8 mean absolute CWT coefficients of AE signals from only one sensor and cutting conditions.
4) 2S-DWT: Input 14 DWT level-RMS values of AE signals from two sensors and cutting conditions.
5) 2S-CWT: Input 16 mean absolute CWT coefficients of AE signals from two sensors and cutting conditions.
6) 2S-All: Input 14 DWT level-RMS values and 16 mean absolute CWT coefficients of AE signals from two sensors and cutting conditions.

5. Results and Discussion

The tool wear curve in Fig. 8 shows patterns of the flank wear at different cutting speeds and feeds, as a function of cutting length. The cutting length is the accumulated depth of holes drilled during each test. The V_B values show faster flank wear and shorter drill life with higher cutting speed and feed. However, the relationship between the AE signal and drill wear is not simple. Therefore the drill wear estimated from the extracted features of AE signal were analyzed by neural network which are non-linear mapping models. For cutting conditions used in training and testing phase, each drilling test forms a pattern of input and output parameters; such 483 patterns were used in the training and testing phases. Out of 483 patterns, 438 patterns are chosen randomly for training the network and others for testing (simulating) the neural network. Based on the aforementioned neural network model for this study, number of neurons to be used in the hidden layers of a neural network is critical in order to avoid underfitting and overfitting problem. There is no single rule to determine the optimum number of neurons in the hidden layers required for optimum performance. However, number of hidden layer neurons is usually found with trial and error approach.

In this study, the number of neurons in hidden layers was determined by a trial-and-error approach. Each network architecture was testified for the average MSE of 5 trials with the number of neurons 4, 6, 8, 10 in first hidden layer and the number of neurons from two (2) to ten (10) in second layer and the minimum value out of 36 average MSE determined the number of neurons. The number of neurons for trial and error is set maximum value at ten neurons in both first and second hidden layers (10-10) because the number of training patterns should be greater than the number of the total synaptic weight to avoid ill-posedness. The Fig. 9 shows the minimum average MSE at the number of hidden neurons 8-10 for neural network architectures 2S-All. Similar approach is repeated for other neural network architectures to determine the number of hidden layer neurons. Consequently, the number of first and second hidden neurons 4-5, 4-7, 8-6, 6-4 and 8-5 are chosen for neural network architectures 1S-DWT,

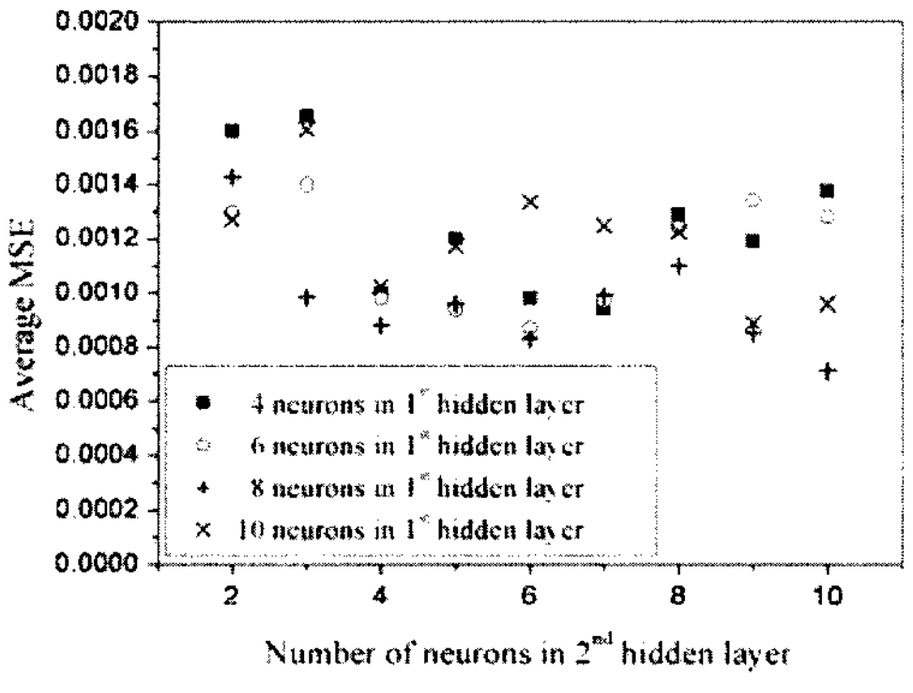

Fig. 9 Average MSE values of neural network architectures 2S-All as a function of the number of neurons in the hidden layers

1S-CWT, 1S-All, 2S-DWT and 2S-CWT, respectively.

Table 1 shows a summary of the performance of the neural networks with different architectures during testing phase. The percentage of correct prediction for each set of drilling conditions is calculated as:

$$Percentage\ of\ Correct\ Prediction = \frac{\sum_{i=1}^{n}\left(1-\frac{\left|x_i^{measured}-x_i^{predicted}\right|}{x_i^{measured}}\right)\times 100}{n} \quad (2)$$

where n is the number of patterns in testing phase, while $x_i^{measured}$ and $x_i^{predicted}$ represent the measured and predicted flank wear of ith pattern in testing phase, respectively. The testing phase helps the neural network architectures to generalize and increase its declaration accuracy. The results indicate that neural networks with input features extracted from two sensors are more accurate than the networks with only one sensor input. The overall average correct predictions indicated that the best performance was obtained by the neural network architecture

Table 1 Performance of neural network with different structures during testing phase

No. of sensor input	Drilling conditions		Percentage of correct predictions		
	Cutting speed (m/min)	Feed (mm/rev)	DWT level-RMS	Mean absolute CWT coeff.	All
One Sensor	22	0.13	81.87	78.64	85.79
	22	0.15	76.52	77.06	83.54
	22	0.17	84.13	83.36	87.26
	26	0.13	78.92	76.24	84.32
	26	0.15	76.58	80.51	84.95
	26	0.17	69.72	76.98	75.46
	30	0.13	80.76	79.52	80.87
	30	0.15	79.73	81.79	82.75
	30	0.17	82.38	79.68	84.86
	Average		78.96	79.31	83.31
One Sensor*	24	0.18	72.64	72.39	75.79
	28	0.14	71.51	76.36	80.72
	32	0.12	75.85	73.57	76.97
	Average		73.33	74.11	77.83
Overall average			77.55	78.01	81.94
Two Sensors	22	0.13	87.35	90.48	94.59
	22	0.15	84.93	87.79	91.67
	22	0.17	79.38	83.64	88.78
	26	0.13	91.03	89.89	94.37
	26	0.15	78.37	79.85	84.42
	26	0.17	84.69	85.59	87.62
	30	0.13	86.85	89.38	91.93
	30	0.15	84.76	83.62	88.46
	30	0.17	83.79	80.67	86.83
	Average		84.57	85.66	89.85
Two Sensors*	24	0.18	87.14	83.75	91.43
	28	0.14	83.85	85.92	85.21
	32	0.12	79.24	80.73	87.68
	Average		83.41	83.47	88.11
Overall average			84.28	85.11	89.42

*Untrained data sets; Signals from these conditions were not used in the training phase

with input features from two sensors and both of the wavelet transforms, i.e. 2S-All. The performance of the architecture with input features by CWT is slightly higher than that by DWT, but the difference was almost negligible and within the range of statistical error bound.

In order to further verify the feasibility of using neural networks for the diagnosis of drill wear, the six architectures were tested with untrained data sets that were acquired under the drilling conditions different from those used for training the neural networks. The performance of three architectures with two sensors input was satisfactory, although it was less accurate than the performance for the cutting conditions used for training. When the performance of three architectures was tested with the input features from only one sensor input, the difference in the percentage of correct prediction between trained and untrained became much larger. Because the drilling position moved around within specimens, the distance from cutting source location to the sensor varied with the drilling of every hole. AE signal amplitude decreased in amplitude with the distance from source to sensor due to attenuation, which might affect the quality of input features extracted from the signal. This effect became less significant when the input features were extracted from the signals acquired by two sensors.

6. Conclusions

A multi-layer feed-forward neural network with back-propagation training algorithm was developed and applied to AE signal analysis to be used for drill wear monitoring. The performance of six different neural network architectures was tested and found to be sensitive to the type of input data. The combination of DWT level-RMS voltage and mean absolute CWT coefficients as the input features resulted in the best performance to predict about the drill wear condition. In addition, neural networks with input features extracted from two sensors are more accurate than the networks with only one sensor input. These provided the 2S-All neural network architecture to obtain the best performance at a correct prediction of 89.4%. The results showed that once the neural network was properly trained, it could be a powerful and reliable tool to solve the classification and pattern recognition problems of such AE signals as being acquired in the tool condition monitoring applications.

Acknowledgement

The authors gratefully acknowledge Professor Cho, Myeong-Woo at Inha University for his kind advice and help in using the machining facility.

References

Abu-Mahfouz, Issam (2005) Drill Flank Wear Estimation Using Supervised Vector Quantization Neural Networks, Neural Computing & Applications, Vol. 14, pp. 167-175

Demuth, Howard and Beale, Mark (1998) Neural Network Toolbox User's Guide, Version 3.0, Natick, MA, USA, The Math works, Inc.

Kim, S. H. and Lee, K. Y. (2001) Development of Defect Classification Program by Wavelet Transform and Neural Network and Its Application to AE Signal Due to Welding Defect, Journal of the Korean Society for Nondestructive Testing, Vol. 21, No. 1, pp. 54-61

Lee, K. J., Kwon, O. Y. and Joo, Y. C. (2000) An Improved AE Source Location by Wavelet Transform De-Noising Technique, Journal of the Korean Society for Nondestructive Testing, Vol. 20, No. 6, pp. 490-500

Li, Xiaoli and Patri, K. V. (1999) Wavelet Packet Transforms of Acoustic Emission Signals for Tool Wear Monitoring, Int. J. Manufacturing Science & Technology, Vol. 1, No. 2, pp. 89-93

Li, Xiaoli and Wu, J. (2000a) Wavelet Analysis of Acoustic Emission Signals in Boring, Proceeding of the Institute of Mechanical Engineers Part B Vol. 214, No. 5, pp. 421-424

Li, Xiaoli (2002) A Brief Review: Acoustic Emission Method for Tool Wear Monitoring During Turning, Int. J. Machine Tools & Manufacture Vol. 42, pp. 157-165

Misiti, M., Misiti, Y., Oppenheim, G. and Poggi, J. M. (2000) Wavelet Toolbox User's Guide, Version 2.0, Natick, MA, USA, The Math works, Inc.

Patra, K., Pal, S. K. and Bhattacharyya, K. (2007) Artificial Neural Network Based Prediction of Drill Flank Wear from Motor Current Signals, Applied Soft Computing, Vol. 7, pp. 929-935

Singh, A. K., Panda, S. S., Pal S. K. and Chakraborty D. (2006) Predicting Drill Wear Using an Artificial Neural Network, Int. J. Adv. Manufacturing Technology, Vol. 28, pp. 456-462

Sun, J., Hong, G. S., Rahman, M. and Wong, Y.S. (2004) Identification of Feature Set for Effective Tool Condition Monitoring by Acoustic Emission Sensing, Int. J. Production Research Vol. 42, No. 5, pp. 901-918